Effect of surface roughness on the self-assembly of octadecanethiol monolayer onto polycrystalline noble metal surfaces

R. Subramanian and V. Lakshminarayanan

Raman Research Institute, Bangalore 560 080, India

The role of surface roughness on defect formation in ocatadecanethiol monolayer covered surfaces of gold, silver and copper has been investigated using cyclic voltammetry and scanning tunneling microscopy. The adsorption of alkanethiol on surfaces subjected to various pre-treatments like mechanical polishing using different grades of emery and alumina indicates that a surface polished with 0.05 µm alumina has a significantly greater number of defect sites, thereby allowing access to redox species, compared to a surface treated with coarse emery. Scanning tunneling microscopic studies reveal that for a given area, a 'smooth' alumina polished surface has a number of closely spaced corrugations compared to a surface roughened using a coarse emery. From these results, we establish that there exists a direct correlation between surface roughness and barrier efficiency.

Long chain alkanethiols chemisorb strongly and form highly ordered and stable self-assembled monolayers on different metal surfaces such as copper[1–6], silver[7,8] and gold[9–13]. One of the important properties of an alkanethiol monolayer is its binding to an electrode surface and the inhibiting behaviour of the resulting monolayer film to electron transfer reaction. This is because of the fact that the film acts as a physical barrier between the electrode surface and the ions in the solution[14–17]. The barrier property and hence the quality of the monolayer is usually evaluated from the defects that are present. This can be ascertained electrochemically by carrying out cyclic voltammetry of the metal oxidation–reduction reaction on a monolayer covered surface.

We find from the literature that Creager *et al.*[18] have studied the effect of chemical etching on the blocking nature of alkanethiol monolayer on gold. They report that the monolayer formed on gold etched in aqua regia was better than that on evaporated gold thin films. By scanning tunneling microscopic studies, they showed that the aqua regia-treated surface was, in fact, microscopically smoother compared to evaporated gold surface which therefore helped in the formation of an effective barrier film. On the contrary, Guo *et al.*[19] treated the gold substrate prior to adsorption of thiol at different temperatures and report that the pinhole defect density is largest for an atomically smooth surface formed at the highest temperature they used. To resolve this issue, we thought it worthwhile to carry out a systematic study of the octadecanethiol monolayer by introducing mechanically controlled roughness on the substrates, and examine the role of surface roughness on the barrier properties of the thiol. The advantage of this approach is that not only can one control the extent of roughness created on the surface, but also vary the same to study if there is any correlation between the substrate roughness and the defect formation in the monolayer. We have used cyclic voltammetry to study the defect formation and structural stability while the role of surface morphology was examined by scanning tunneling microscopy.

We study the effect of mechanical polishing, by varying the particle size of the polishing materials. The topography of the substrate is thus changed in a controlled manner during each treatment and the corresponding roughness factor determined for gold by cyclic voltammetry[20]. The blocking nature of the self-assembled monolayers on the metal electrodes is determined by cyclic voltammetry of the respective metal oxidation and reduction reaction in alkaline media. We have used this method of characterizing the film because: (i) It is reported in the literature[21] that the oxide stripping current affords a quick assessment of the area fraction of the pinholes since the oxidation of the metal can occur only if the redox species (hydroxyl ion in this case) reach the electrode surface through the pinholes. Hence, the measured charge from the area under the peak is indicative of defect sites in the monolayer. (ii) All the three metals studied exhibit well-defined and reproducible oxidation–reduction peaks in alkaline medium.

For the cyclic voltammetric measurements, gold, silver and copper specimens of >99.9% purity were used in the form of metal strips. A well-defined region of the electrode was exposed to the electrolyte, the remaining portion being well insulated with Parafilm, a self-sealing inert thermoplastic (American National Can) and then with Teflon. The geometric area of the electrodes exposed to the electrolytes was about 1 cm^2. Before each experiment, the actual geometric area was measured and it generally ranged within 5% of this value. The metal surface was then hand polished with emery papers of the grades 800, 1000 and 1500 (3M make) whose particle sizes are 17 µm, 13 µm and 9 µm respectively[22]. The electrodes after polishing were rinsed in distilled water, sonicated and immediately immersed in 1 mM octadecanethiol (Aldrich) in ethanol for 30 min. Alumina-treated specimens were prepared by first polishing them with emery, followed by polishing successively on a microcloth having a slurry of 1, 0.3, 0.05 µm alumina powder (Buehler).

*For correspondence. (e-mail: narayan@rri.ernet.in)

A conventional three-electrode electrochemical cell was used for the cyclic voltammetric studies. The counter electrode was a platinum strip of sufficiently large surface area. All the potentials were measured against Hg/Hg_2SO_4 (saturated Na_2SO_4) reference electrode. All the experiments were conducted in an atmosphere of oxygen-free nitrogen gas. The electrolyte was 0.1 M NaOH prepared in Millipore water. Cyclic voltammetry was carried out using an EG&G potentiostat (Model 263A) interfaced to a PC through a GPIB card (National Instruments). Charge measurements were carried out from the first scan CV in each case. For copper and silver, the cyclic voltammetric measurements were carried out at a scan rate of 20 mV/s while for gold the scan rate used was 100 mV/s. The real surface area of gold was determined by cyclic voltammetry, using the cathodic stripping peak of gold in 0.5 M sulphuric acid obtained at a scan rate of 100 mV/s and scan range of – 610 mV to 1000 mV vs sulphate electrode.

Scanning tunneling microscopic studies were carried out in air on the mechanically polished gold surface before and after formation of monolayers. The gold samples were immersed in 1 mM octadecanethiol in ethanol solution for 30 min and washed in ethanol and dried to be immediately mounted on the STM sample holder for imaging. A home made STM[22] operating in constant current mode was used for measurement. This was calibrated by imaging with a highly oriented pyrolytic graphite (HOPG) surface before the experiments. The images shown are of raw data without any filtering. However, plane tilt correction was carried out. The images are obtained using the IDL (5.0.2) software (Research System Inc., USA). Electrochemically etched tungsten tip was used as a probe. The tunneling current for imaging the bare surface was 1 nA at a bias voltage of 100 mV while for the thiol adsorbed surface, tunneling current was 200 pA at the same bias voltage. STM imaging was carried out at different regions of the surface and at several scan ranges to verify the overall reproducibility of the surface features.

Figures 1 *a*, 2 *a* and 3 *a* show the cyclic voltammograms in 0.1 M NaOH of bare gold, silver and copper

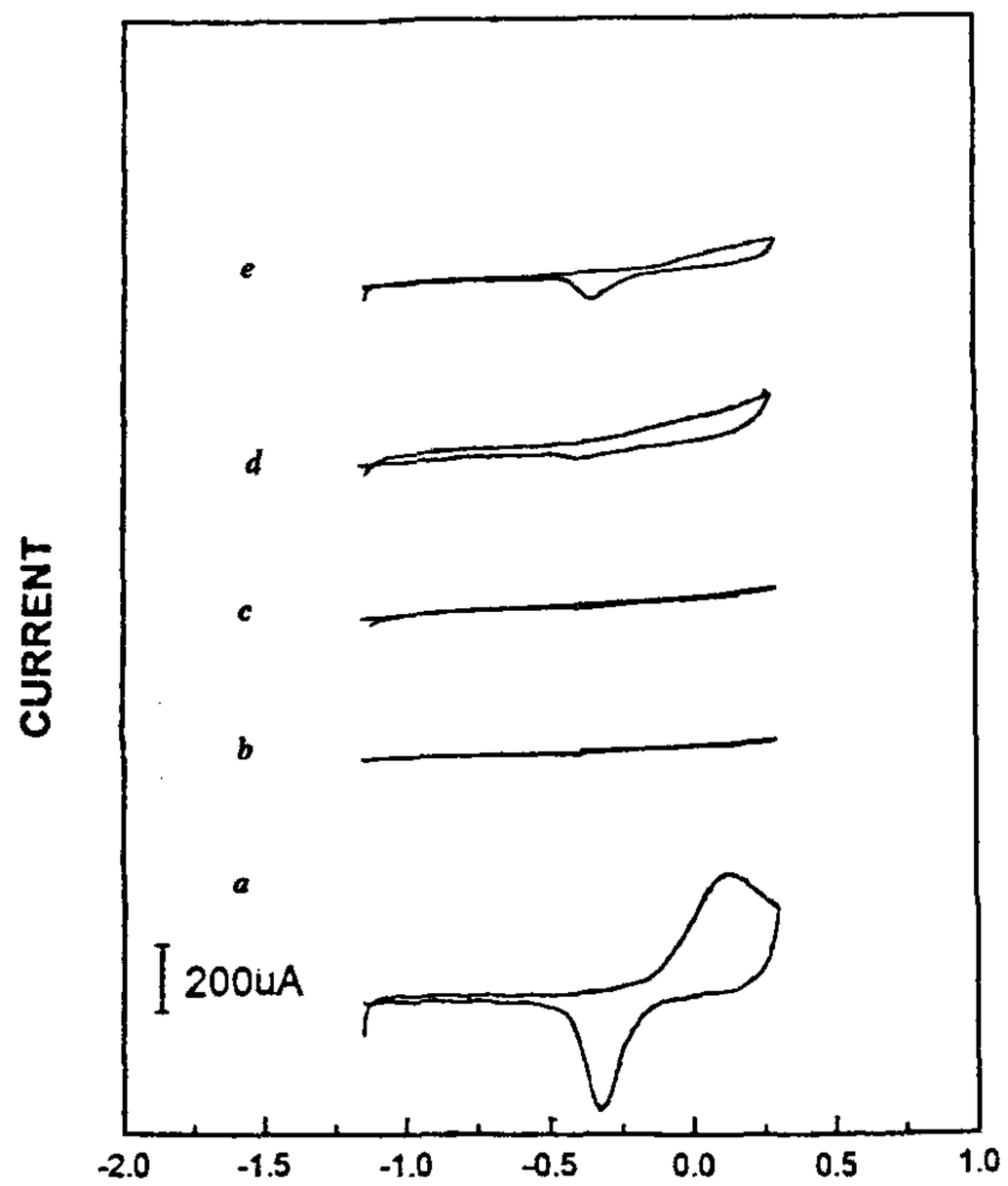

Figure 1 *a–e*. CVs of Au in 0.1 M NaOH, scan rate is 100 mV/s, scan range is – 1.15 V to 0.3 V and electrode area is 1.06 cm^2. *a*, Bare electrode (without dipping in thiol); *b–e*, After pretreatment and dip in 1 mM octadecanethiol for 30 min; *b*, Pre-treated with 800 grade emery (17 µm particle size), electrode roughness factor = 2.204; *c*, Pre-treated with 1000 grade emery (10 µm particle size), electrode roughness factor = 2.137; *d*, Pre-treated with 1500 grade emery (9 µm particle size), electrode roughness factor = 2.035; *e* Pre-treated with 0.05 µm alumina particle, electrode roughness factor = 1.775. Potentials are referred with respect to $Hg \mid Hg_2SO_4$, sat Na_2SO_4 electrode.

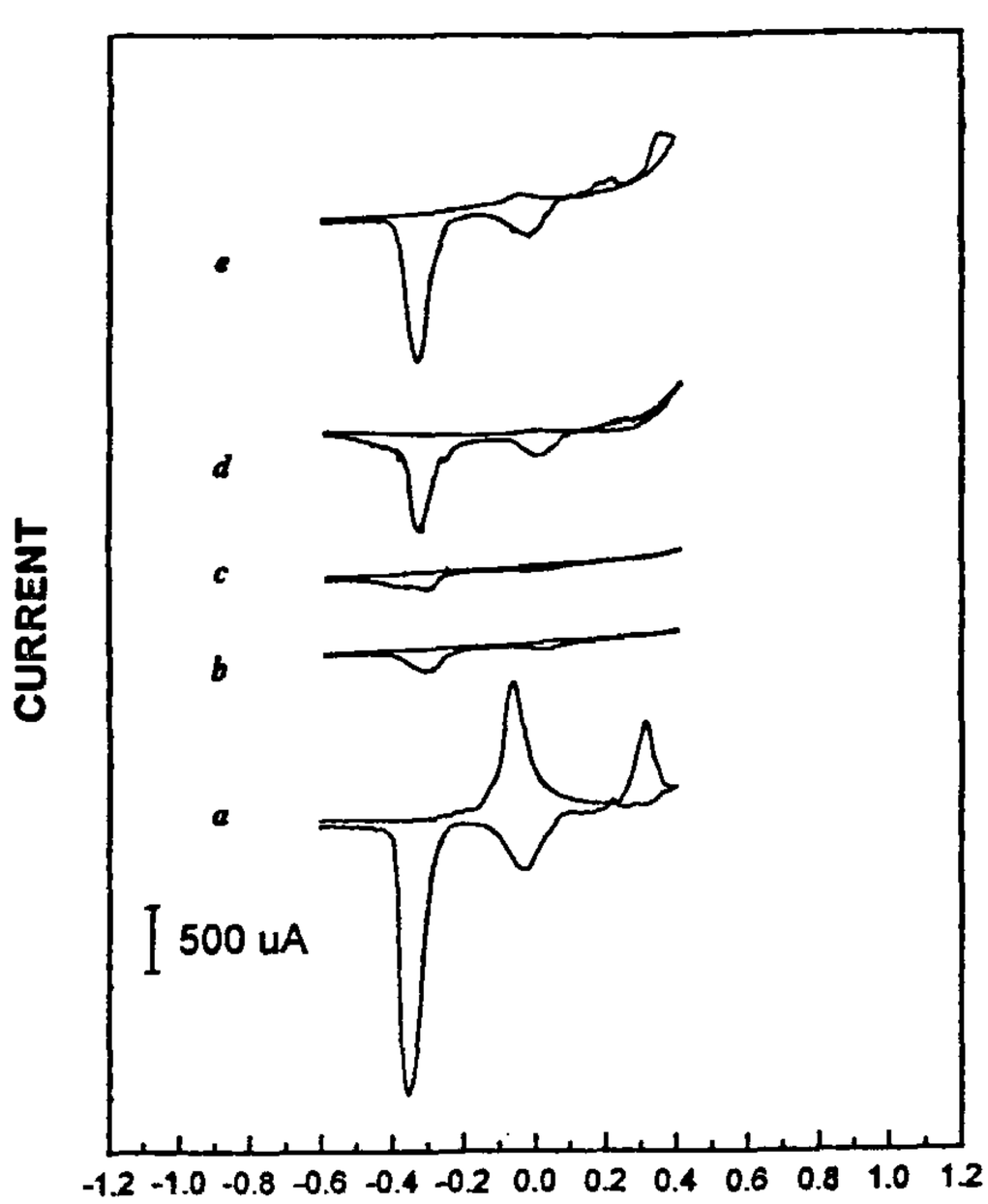

Figure 2 *a–e*. CVs of Ag in 0.1 M NaOH, scan rate is 20 mV/s, scan range is – 0.6 V to + 0.4 V and electrode area is 0.82 cm^2. *a*, Bare electrode (without dipping in thiol); *b*, After treating with 800 grade emery (17 µm particle) and 30 min dip in 1 mM octadecanethiol; *c*, After treating with 1000 grade emery (13 µm particle) and 30 min dip in 1 mM octadecanethiol; *d*, After treating with 1500 (9 µm particle) grade emery and 30 min dip in 1 mM octadecanethiol; *e*, After treating with 0.05 µm alumina and 30 min dip in 1 mM octadecanethiol. Potentials are referred with respect to $Hg \mid Hg_2SO_4$, sat Na_2SO_4 electrode.

electrodes polished with 0.05 μm alumina particles. The cyclic voltammograms (CVs) were taken after 15 min of immersion and at room temperature. The CV of copper in 0.1 M NaOH solution shows three anodic and two cathodic peaks. It is reported that the first anodic peak corresponds to the oxidation of Cu to Cu_2O monolayer formation[23]. The second and third peaks have been ascribed to the multilayer formation of CuO in parallel pathways, viz. oxidation of Cu_2O to CuO and another directly from Cu by two electron transfers[23]. In the reverse scan, the fourth peak corresponds to the cathodic reduction of CuO to Cu_2O while the fifth one is due to the reduction of Cu_2O to Cu. The CV of silver in 0.1 M NaOH also shows the presence of two prominent anodic and cathodic peaks corresponding to the formation of Ag_2O and AgO (ref. 24). In the case of gold[25] there is a single anodic peak corresponding to the formation of a monolayer of oxygen atoms. During the cathodic scan the peak corresponds to the stripping of adsorbed oxygen.

Figures 1 *b–f*, 2 *b–f* and 3 *b–f* show the CVs of octadecanethiol covered gold, silver and copper electrodes

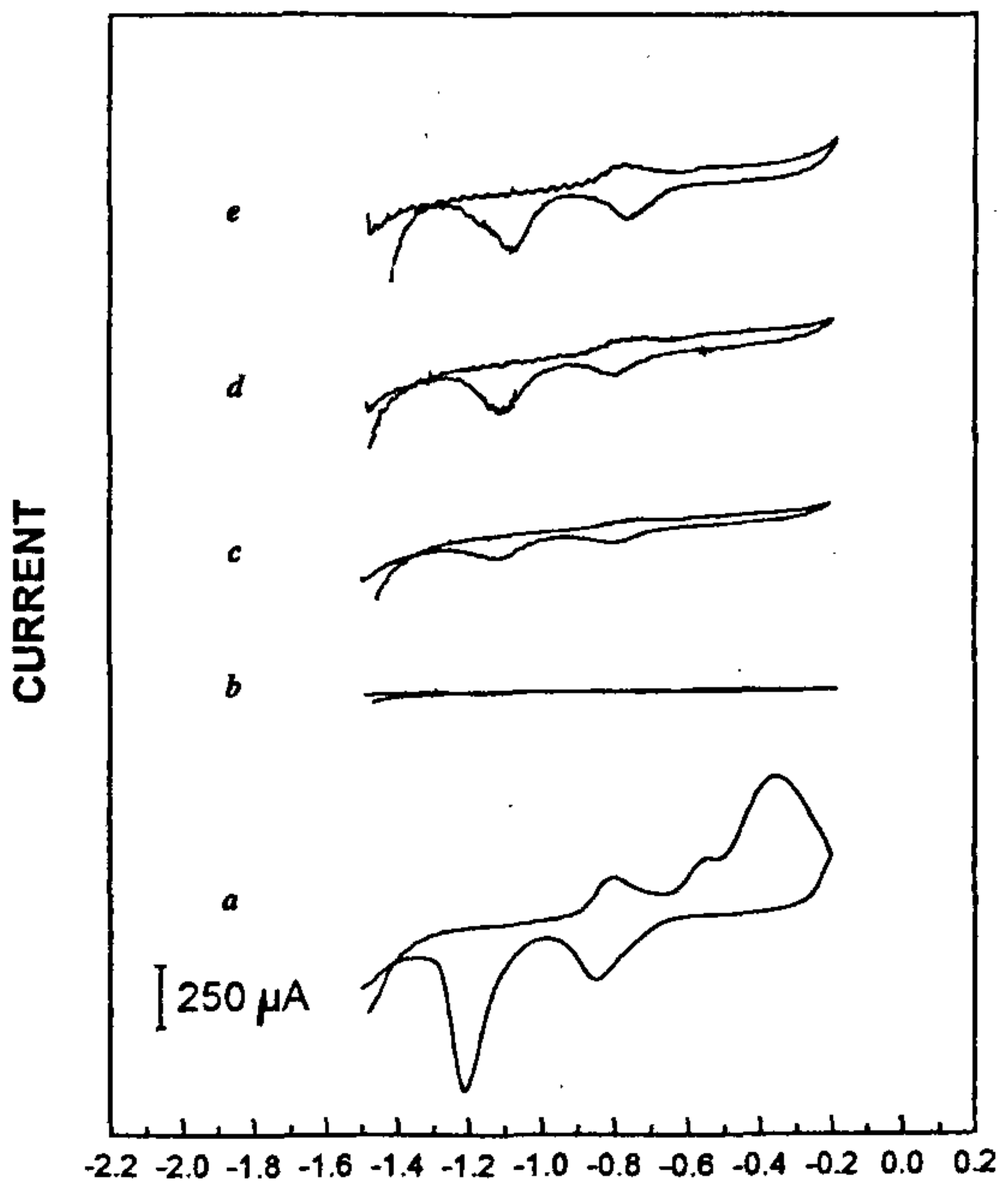

Figure 3 *a–e*. CVs of Cu in 0.1 M NaOH, scan rate is 20 mV/s, scan range is −1.5 V to −0.2 V and electrode area is 0.98 cm^2. *a*, Bare electrode (without dipping in thiol); *b*, After treating with 800 grade emery (17 μm particle) and 30 min dip in 1 mM octadecanethiol; *c*, After treating with 1000 grade emery (13 μm particle) and 30 min dip in 1 mM octadecanethiol; *d*, After treating with 1500 grade emery (9 μm particle) and 30 min dip in 1 mM octadecanethiol; *e*, After treating with 0.05 micron alumina and 30 min dip in 1 mM octadecanethiol. Potentials are referred with respect to $Hg|Hg_2SO_4$, sat Na_2SO_4 electrode.

in 0.1 M NaOH for different surface pre-treatments. There is a marked decrease in the peak heights in all the cases *vis-à-vis* respective bare electrode which obviously is due to the physical barrier formed by octadecanethiol monolayer that inhibits electron transfer reaction. It can also be seen that in the case of silver and copper the anodic peaks are less prominent and rather drawn out than the cathodic peaks after thiol adsorption. There is also a shift in the peak potentials towards more positive values after the thiol adsorption. These observations show that there is a change in the nature of oxide formation and oxygen chemisorption on the metal covered with octadecanethiol.

Measurement of charge involved in the redox reaction, by integrating the voltammetric peaks provides an estimate of the extent of electrochemical reaction taking place on the surface. Table 1 shows the charges measured for different mechanically treated surfaces, by integrating both the cathodic peaks in the case of Cu and Ag and the only cathodic peak in the case of Au. The blank values (without thiol adsorption) are shown only for alumina-polished surfaces for comparison. From the table, it can be clearly seen that the integrated charge measured on an alkanethiol adsorbed surface increases quite significantly with the decreasing particle size of the abrasive used for polishing. This shows that a surface roughened with 17 μm blocks the charge transfer reaction more effectively than a surface treated with a 0.05 μm alumina surface. In fact, in the case of gold, for the surfaces treated with 17 μm and 13 μm particles the CVs are just straight lines and the charges are hardly measurable at a slower scan rate of 20 mV/s. Hence we have used a higher scan rate of 100 mV/s in this case.

We have determined the fractional coverage of the octadecanethiol adsorption on gold using the integrated

Table 1. Cathodic charges (in mC/cm^2) measured from the CVs for the blank electrode (alumina polished and without thiol adsorption) and surfaces subjected to different pre-treatments followed by thiol adsorption

Pre-treatment*	Copper	Silver	Gold
Blank (thiol free)	8.75	11.77	0.696
800 Emery (17 μm)	0.36	0.66	0.018
1000 Emery (13 μm)	1.55	1.13	0.018
1500 emery (9 μm)	2.13	4.25	0.049
Alumina polishing (0.05 μm)	3.76	6.91	0.148

*The values given in the parenthesis are the particle sizes of the abrasives used.

Table 2. Fractional coverage of octadecanethiol monolayer on copper, silver and gold surfaces treated with abrasives of different particle sizes

Particle size	17 μm	13 μm	9 μm	0.05 μm
Copper	95.8%	82.2%	75.6%	57%
Silver	94.4%	90.3%	63.9%	41.3%
Gold	97.4%	97.4%	92.9%	78.5%

charges. Though this is only an indirect and semi quantitative method, it provides a quick and convenient way of estimating the relative coverage on different pre-treated surfaces. Table 2 shows the fractional coverage of the octadecanethiol on copper, silver and gold surfaces when polished with particles of different sizes. These values are obtained from the formula:

$$\text{Fractional coverage} = \frac{Q_B - Q_T}{Q_B} \times 100,$$

where Q_T and Q_B respectively are the integrated cathodic charges of the octadecanethiol adsorbed surface and bare metal surface for each of the polishing treatments. For copper and silver, charge values are calculated using the integrated charges of both the peaks of anodic and cathodic cycles. From the table it is clear that the fractional coverage decreases with the decreasing particle size of the abrasive used. This change is also most pronounced in the case of alumina-polished surface. In other words, the surface polished with alumina is least effective as a barrier for faradaic reaction compared with the one with 800 grit emery. This also clearly establishes a direct correspondence between the efficiency of the barrier film and the surface roughness.

Our observation of increase in coverage with increasing roughness is rather surprising and has an important bearing on the SAM formation on mechanically treated surfaces. Therefore we first studied how real surface area changes with polishing. For this, the real surface area of gold was measured from the standard electrochemical procedure of measuring integrated cathodic charge corresponding to the cathodic stripping of oxide on the bare metal electrode assuming charge per unit area as 400 $\mu C/cm^2$. We find from these measurements that the real surface area increases, but not considerably, with increasing roughness of the emery used for treatment. For example, the roughness factor (i.e. real area/geometric area) for surfaces treated with 0.05 µm alumina, 1500, 1000 and 800 emery are 1.775, 2.035, 2.137, 2.204 respectively. This shows that increase in the real surface area from the smoothest (0.05 µm) polishing material to coarsest (17 µm particle emery) is only to the extent of 25%. However, from Table 2, it can be seen that the surface treated with coarse particle of 17 µm has a defect region of about 2.6% of the total area compared to 21.5% in the case of surface polished with fine alumina particle. An explanation for this order of magnitude increase in the defect regions is sought from the scanning tunneling microscopy (STM) studies on the surface of gold and the results are discussed below.

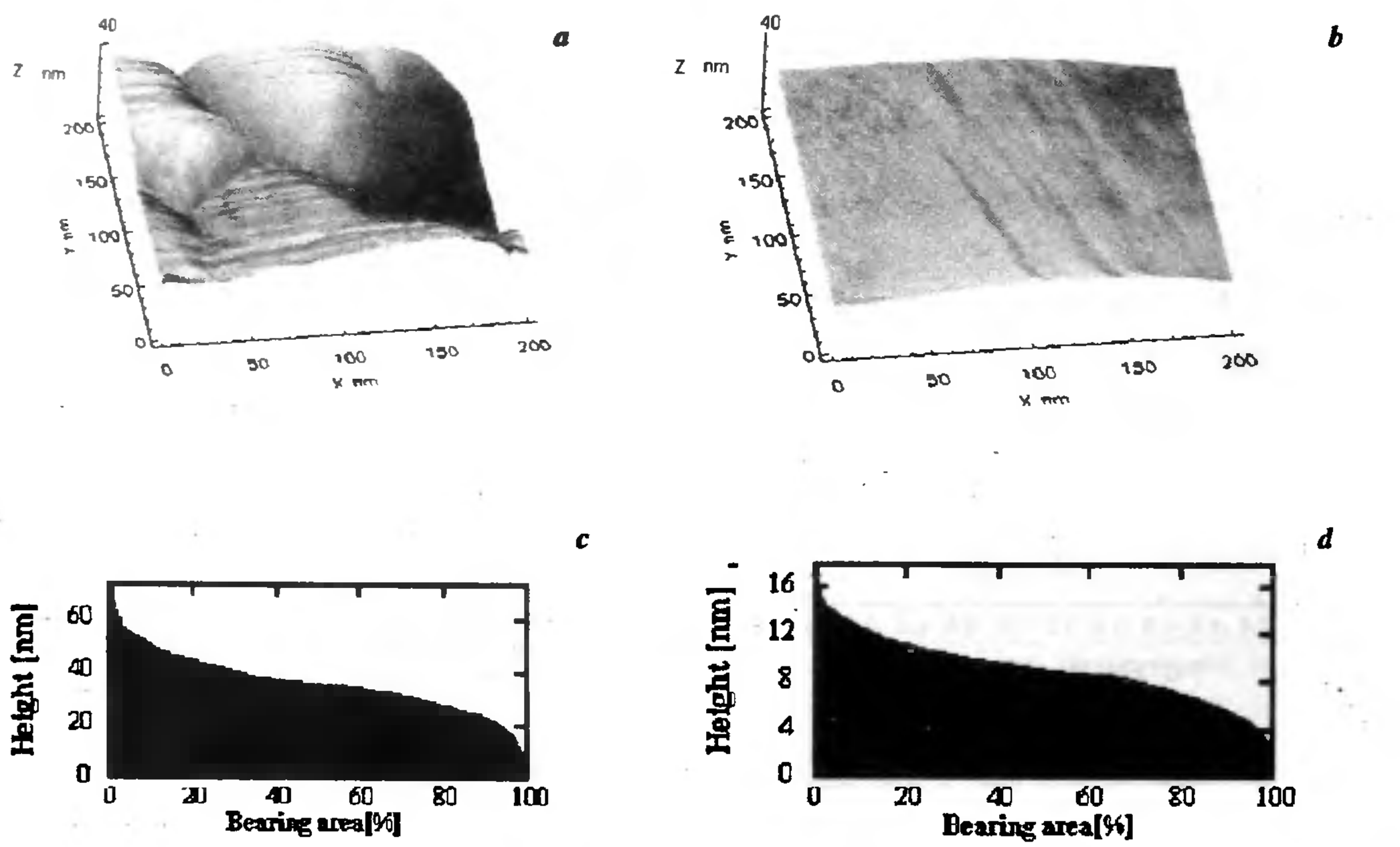

Figure 4 *a–d*. *a*, STM image of polycrystalline gold surface polished with 0.05 µm alumina; *b*, STM image of polycrystalline gold surface polished with 800 grade emery (17 µm particle size); *c*, Abbot curve showing the surface height as a function of the total surface area for the surface polished with 0.05 µm alumina; *d*, Abbot curve showing the surface height as a function of the total surface area for the surface treated with 17 µm particle emery.

Figure 4 *a*, *b* shows the typical 200 nm × 200 nm STM images of gold surface after polishing with 0.05 μm alumina and 17 μm particle emery respectively. The alumina polished surface which appears smooth and bright visually and through an optical microscope can be seen to be granular with several nm level corrugations. Each such region is approximately 30 nm in height and 60–80 nm in diameter. The surface treated with 17 μm particle emery paper is surprisingly smooth on the same scale without similar regions of roughness and steps of comparable size. Figure 4 *c*, *d* shows the Abbott curves, where the surface heights are plotted as a function of percentage of total true area. These curves show the roughness distribution on the surface of alumina polished and the 17 μm particle-treated surfaces respectively. It can be seen that the surface polished with emery has surface roughness of maximum height extending to about 12 nm while an alumina-treated surface has a much higher degree of roughness extending to more than about 50 nm on the same scale. The thiol covered surfaces (not shown in the figures) also exhibit similar features as the bare surface indicating that the adsorbed thiol molecules do not alter the surface features at nm scale to any significant extent.

From the above results we infer that the defects are predominantly formed on the surface corrugation regions. These regions, which are present in large numbers on alumina-polished surface provide the redox species (hydroxyl ions in this case) access to reach the electrode. As the particle size of the emery used for polishing increases, the surface appears smoother at nm level and rougher at a much larger scale. Apparently, large-sized particles simply bulldoze their way on the surface, creating wider grooves even while obliterating smaller hills and valleys. Consequently, this results in lesser number of defect sites on such a surface that is reflected in lower charge values and hence better coverage. The behaviour exhibited by the alkanethiol covered electrodes is remarkably similar in the case of all the three metals studied in this work.

Our results clearly establish for the first time, that there exists a direct correlation between the surface roughness and barrier efficiency. We believe that these results and methodology adopted in this work will contribute to a better understanding of the role of surface roughness on the barrier properties of self-assembled monolayers.

1. Ulman, A., *An Introduction to Ultrathin Organic Films. From Langmuir–Blodgett to Self-Assembly*, Academic Press, Boston, 1991.
2. Yiqi Feng, Wah-Koon Teo, Kok-Siong Siow, Zzhiqiang Gao, Kuan Lee Tan and An-Kong Hseih, *J. Electrochem. Soc.*, 1997, **144**, 55–64.
3. Laibinis, P. E., Bain, C. D. and Whitesides, G. M., *J. Phys. Chem.*, 1991, **95**, 7017–7021.
4. Laibinis, P. E., Whitesides, G. M., Allara, D. L., Tao, Y. T., Parikh, A. N. and Nuzzo, R. G., *J. Am. Chem. Soc.*, 1991, **113**, 7152–7167.
5. Yamamoto, Y., Nishihara, H. and Aramaki, K., *J. Electrochem. Soc.*, 1993, **140**, 436–443.
6. Ishibashi, M., Itoh, M., Nishihara, H. and Aramaki, K., *Electrochim. Acta*, 1996, **41**, 241–248.
7. Walczak, M. M., Chung, C., Stole, S. M., Widrig, C. A. and Porter, M. D., *J. Am. Chem. Soc.*, 1991, **113**, 2370–2378.
8. Widrig, A., Chung, C. and Porter, M. D., *J. Electroanal. Chem.*, 1991, **310**, 335–359.
9. Nuzzo, R. G. and Allara, D. L., *J. Am. Chem. Soc.*, 1983, **105**, 4481–4483.
10. Strong, L. and Whitesides, G. M., *Langmuir*, 1988, **4**, 546–558.
11. Porter, M. D., Bright, T. B., Allara, D. L. and Chidsey, C. E. D., *J. Am. Chem. Soc.*, 1987, **109**, 3559–3568.
12. Jie Xu and Hu-Lin Li, *J. Colloid Interface Sci.*, 1995, **176**, 138–149.
13. Bain, C. B. and Whitesides, G. M., *J. Am. Chem. Soc.*, 1988, **110**, 5897–5898.
14. Sabatini, E. and Rubinstein, I., *J. Phys. Chem.*, 1987, **91**, 6663–6669.
15. Chidsey, C. E. D. and Loiacono, D. N., *Langmuir*, 1990, **6**, 682–691.
16. Finklea, H. O., Snider, D. A., Fedyk, J., Sabatini, E., Gafni, Y. and Rubinste, I., *Langmuir*, 1993, **9**, 3660–3667.
17. Finklea, H. O., Snider, D. A. and Fedyk, J., *Langmuir*, 1990, **6**, 371–376.
18. Creager, S. E., Hockett, L. A. and Rowe, G. K., *Langmuir*, 1992, **8**, 854–861.
19. Guo, L. H., Facci, J. S., McLendon, G. and Mosher, R., *Langmuir*, 1994, **10**, 4588–4593.
20. Trasatti, S. and Petrii, O. A., *Pure Appl. Chem.*, 1991, **63**, 711–734.
21. Finklea, H. O., in *Electroanalytical Chemistry. A Series of Advances* (eds Bard, A. J. and Rubinstein, I.), Marcel Dekker Inc., New York, 1996, vol. 19, pp. 124 and 166.
22. Lakshminarayanan, V., *Curr. Sci.*, 1998, **74**, 413–417.
23. Abd El Halcem, S. M. and Ateya, B. G., *J. Electroanal. Chem.*, 1981, **117**, 309–319.
24. Dirske, T. P., *Electrochim. Acta*, 1989, **34**, 647–650.
25. Hamelin, A., Sottomayor, M. J., Silva, F., Si-Chung Chang and Weaver, M., *J. Electroanal. Chem.*, 1990, **295**, 291–300.

Received 26 November 1998; revised accepted 2 February 1999